LETTER **Communicated by Thomas Kreuz**

Comparison of Different Spike Train Synchrony Measures Regarding Their Robustness to Erroneous Data From Bicuculline-Induced Epileptiform Activity

Manuel Ciba
manuel.ciba@th-ab.de
Robert Bestel
robert.bestel@mailbox.org
Christoph Nick
christoph.nick@web.de
Biomems Lab, University of Applied Science Aschaffenburg, 63743 Aschaffenburg, Germany

Guilherme Ferraz de Arruda
gui.f.arruda@gmail.com
ISI Foundation, 10126 Turin, Italy

Thomas Peron
thomaskaue@gmail.com
Institute of Mathematics and Computer Science, University of São Paulo, São Carlos SP 13566-590, Brazil

Comin César Henrique
chcomin@gmail.com
Department of Computer Science, Federal University of São Carlos, São Carlos SP 13565-905, Brazil

Luciano da Fontoura Costa
ldfcosta@gmail.com
Instituto de Física de São Carlos, University of São Paulo, São Carlos SP 13566-590, Brazil

Francisco Aparecido Rodrigues
francisco.rodrigues.usp@gmail.com
Institute of Mathematics and Computer Science, University of São Paulo, São Carlos SP 13566-590, Brazil

Christiane Thielemann
Christiane.Thielemann@th-ab.de
Biomems Lab, University of Applied Science Aschaffenburg, 63743 Aschaffenburg, Germany

Neural Computation **32, 887–911** (2020)
https://doi.org/10.1162/neco_a_01277

As synchronized activity is associated with basic brain functions and pathological states, spike train synchrony has become an important measure to analyze experimental neuronal data. Many measures of spike train synchrony have been proposed, but there is no gold standard allowing for comparison of results from different experiments. This work aims to provide guidance on which synchrony measure is best suited to quantify the effect of epileptiform-inducing substances (e.g., bicuculline, BIC) in in vitro neuronal spike train data. Spike train data from recordings are likely to suffer from erroneous spike detection, such as missed spikes (false negative) or noise (false positive). Therefore, different timescale-dependent (cross-correlation, mutual information, spike time tiling coefficient) and timescale-independent (Spike-contrast, phase synchronization (PS), A-SPIKE-synchronization, A-ISI-distance, ARI-SPIKE-distance) synchrony measures were compared in terms of their robustness to erroneous spike trains. For this purpose, erroneous spike trains were generated by randomly adding (false positive) or deleting (false negative) spikes (in silico manipulated data) from experimental data. In addition, experimental data were analyzed using different spike detection threshold factors in order to confirm the robustness of the synchrony measures. All experimental data were recorded from cortical neuronal networks on microelectrode array chips, which show epileptiform activity induced by the substance BIC. As a result of the in silico manipulated data, Spike-contrast was the only measure that was robust to false-negative as well as false-positive spikes. Analyzing the experimental data set revealed that all measures were able to capture the effect of BIC in a statistically significant way, with Spike-contrast showing the highest statistical significance even at low spike detection thresholds. In summary, we suggest using Spike-contrast to complement established synchrony measures because it is timescale independent and robust to erroneous spike trains.

1 Introduction

Synchrony is generally accepted to be an important feature of basic brain functions (Engel, Fries, & Singer, 2001; Ward, 2003; Rosenbaum, Tchumatchenko, & Moreno-Bote, 2014) and pathological states (Pare, Curro'Dossi, & Steriade, 1990; Fisher et al., 2005; Truccolo et al., 2014; Arnulfo et al., 2015). Measuring synchrony between neural spike trains is a common method to analyze experimental data, such as recordings from in vitro neuronal cell cultures with microelectrode arrays (MEA; Selinger, Pancrazio, & Gross, 2004; Chiappalone, Bove, Vato, Tedesco, & Martinoia, 2006; Chiappalone, Vato, Berdondini, Koudelka-Hep, & Martinoia, 2007; Eisenman, Emnett, Mohan, Zorumski, & Mennerick, 2015; Flachs & Ciba, 2016) or from in vivo experiments (Li, Doyon, & Dani, 2011). As an example for in

vitro neuronal cell cultures on MEA chips, Sokal, Mason, and Parker (2000) reported that synchrony reliably increased due to the substance bicuculline (BIC), while the usual applied quantification method "spike rate" increased or decreased.

In order to quantify synchrony, many spike train synchrony measures have been proposed based on different approaches. Some of them belong to the class of timescale-dependent measures. This means that at the beginning of the analysis, the user has to select the desired timescale (e.g., bin size) (Selinger et al., 2004; Cutts & Eglen, 2014). The second class contains timescale-independent measures, which automatically adapt their timescale parameter according to the data (Satuvuori et al., 2017; Ciba, Isomura, Jimbo, Bahmer, & Thielemann, 2018). However, there is no gold standard for the evaluation of synchrony in experimental data. This is because there is no common definition of synchrony between spike trains. To be more specific, each synchrony measure can be considered as its own definition of synchrony, extracting different features from the data. This situation is unsatisfactory because data interpretations are not comparable. Therefore, it is desirable to have some guidance on which synchrony measure to use for specific data.

When it comes to the analysis of experimental spike train data, the data are likely to suffer from erroneous spike detection. For example, spikes are missed as they are buried in noise (false negative) or noise is misinterpreted as spikes (false positive). At low signal-to-noise ratios (SNR), even advanced spike detection methods are affected by missed or misinterpreted spikes (Lieb, Stark, & Thielemann, 2017).

Hence, a synchrony measure that operates on spike trains from experimental data should be as robust as possible to such erroneous spike trains.

In order to develop guidance in analyzing epileptiform spike trains from in vitro neuronal networks, the performance of different synchrony measures was compared with the focus on robustness to erroneous spike trains. Well-known timescale-dependent measures like cross-correlation (CC), mutual information (MI), and spike time tiling coefficient (STTC), and timescale-independent measures, like Spike-contrast, phase synchronization (PS), A-SPIKE-synchronization, A-ISI-distance, A-SPIKE-distance, and ARI-SPIKE-distance were applied to two types of data sets: in silico manipulated data and experimental data.

The in silico manipulated data are based on the experimental data and were used to simulate erroneous spike train data by randomly adding spikes (false positive) or deleting spikes (false negative). As a requirement, the synchrony measures should be robust to added and deleted spikes. The experimental data were recorded from primary cortical networks grown in vitro on MEA chips. Neuronal networks were exposed to the γ-aminobutyric acid ($GABA_A$) receptor antagonist BIC in order to increase the synchrony level of the network activity. Spike detection threshold factor was varied in order to vary the level of false-positive and

false-negative spikes. The synchrony measures were tested for their ability to find significant synchrony changes induced by BIC.

2 Material and Methods

2.1 Synchrony Measures. In this section, we briefly describe the synchrony measures used in this study. To consider a wide range of synchronization measures, we chose a representative group of linear and nonlinear methods, as well as timescale-dependent and -independent methods. (For a detailed definition see the respective original publication in the following paragraphs.) Since there is no specific publication on how to apply MI and PS to spike train data, their definitions are provided in the appendix.

We first look at timescale-dependent methods.

• *Cross-correlation* (CC)–based methods are probably most popular to measure synchrony (Cutts & Eglen, 2014). Here we use a definition by Selinger et al. (2004) that was proposed for in vitro experiments and was also used by Chiappalone et al. (2006). According to the definition, synchrony between two spike trains is measured by binning the spike trains into a binary signal and then calculating the cross-correlation without shifting the signals. Selinger et al. (2004) proposed a bin size of 500 ms and was able to detect synchrony changes in spinal cord cultures mediated by the chemicals BIC, strychnin, and 2,3-dioxo-6-nitro-l,2,3,4-tetrahydrobenzoquinoxaline-7-sulphonamide (NBQX). Due to the bin size parameter, CC is timescale dependent. A bin size of 500 ms is also used in this study (see section 2.4).

• *Mutual information* (MI) is a measure from the field of information theory and is, in contrast to CC, able to capture nonlinear dependencies. In this work, MI measures the synchrony between two spike trains by binning the spike trains into binary signals and quantifying the redundant information (Cover & Thomas, 2012). Therefore, this version of MI is timescale dependent using a bin size of 500 ms (see section 2.4).

• *Spike time tiling coefficient* (STTC) measures the synchrony between two spike trains and has been proposed by Cutts and Eglen (2014) as a spike rate–independent replacement of the synchrony measure correlation index by Wong, Meister, and Shatz (1993). Reanalysis of a study of retinal waves using STTC instead of the correlation index significantly changed the result and conclusion (Cutts & Eglen, 2014). STTC is a timescale-dependent measure as it needs a predefined time window Δt in which spikes are considered synchronous. Referring to the work of Cutts and Eglen (2014), we use a time window of 100 ms in this work (see section 2.4).

The timescale-independent methods follow:

• *Phase synchrony* (PS) measures the synchrony between spike trains in two steps. The first step is to assign a linear phase procession from 0 and 2π

to every interspike interval (ISI). The second step is quantifying the common phase evolution of all spike trains via an order parameter defined by Pikovsky, Rosenblum, Osipov, and Kurths (1997). PS is timescale independent and, to the best of our knowledge, has not been systematically compared with other measurements in studies of spike train synchrony yet and has never been used to measure synchrony of neural spike trains.

• *Spike-contrast* is a timescale independent synchrony measure based on the temporal "contrast" of the spike raster plot (activity versus nonactivity in certain temporal bins). It not only provides a single synchrony value, but also a synchrony curve as a function of the bin size—in other words, as a function of the timescale (Ciba et al., 2018). Here, instead of the synchrony curve, only the single synchrony value was used.

• *A-SPIKE-synchronization* is a timescale-independent and parameter-free coincidence detector (Satuvuori et al., 2017). It measures the similarity between spike trains and is the adaptive generalization of SPIKE-synchronization (Kreuz, Mulansky, & Bozanic, 2015). In the adaptive versions, a decision is made if the spike trains are compared considering their local or global timescale, which is advantageous for data containing different timescales, like regular spiking and bursts.

• *A-ISI-distance* is a timescale-independent and parameter-free distance measure (Satuvuori et al., 2017). It measures the instantaneous rate difference between spike trains and is the adaptive generalization of ISI-distance (Kreuz, Haas, Morelli, Abarbanel, & Politi, 2007).

• *A-SPIKE-distance* is a timescale-independent and parameter-free distance measure (Satuvuori et al., 2017). It measures the accuracy of spike times between spike trains relative to local firing rates and is the adaptive generalization of SPIKE-distance (Kreuz, Chicharro, Greschner, & Andrzejak, 2011; Kreuz, Chicharro, Houghton, Andrzejak, & Mormann, 2013).

• *ARI-SPIKE-distance* is the rate-independent version of A-SPIKE-distance (Satuvuori et al., 2017). It measures the accuracy of spike times between spike trains without using the relative local firing rate. Some of the original versions have already been applied to experimental neuronal data. For example Andrzejak, Mormann, and Kreuz (2014) used ISI-distance and SPIKE-distance and Dura-Bernal et al. (2016) used SPIKE-distance and SPIKE-synchronization. Espinal et al. (2016) applied SPIKE-distance to simulated data.

In order to get a final synchrony value over all recorded spike trains, synchrony between all spike train pairs was calculated and averaged. The exception was of Spike-contrast, which already yields a single synchrony value between all spike trains due to its multivariate nature.

Note that all synchrony measures are designed to provide a value between 0 (miminum synchrony) and 1 (maximum synchrony). Only CC and STTC are able to yield negative values in case of anticorrelation. The distance measures A-ISI-distance, A-SPIKE-distance, and ARI-SPIKE-distance

naturally provide values between 0 (minimal distance or maximum synchrony) and 1 (maximum distance or minimum synchrony). Therefore, their values were substracted from 1 to make the distance measures comparable to the synchrony measures. The Matlab (MathWorks, Natick, MA, U.S.A.) source codes of A-SPIKE-synchronization, A-ISI-distance, A-SPIKE-distance, and ARI-SPIKE-distance were downloaded, along with the cSPIKE tool.[1] The Spike-contrast[2] and MI[3] Matlab source code also was taken from online sources. STTC Python code was translated into Matlab code.[4] Matlab code for PS was specifically programmed for this work. All Matlab functions and scripts used for this work are provided online.[5]

2.2 In Silico Manipulated Data. Two sets of in silico manipulated data were generated featuring added spikes (false-positive spikes) and deleted spikes (false-negative spikes). Because the measures CC, MI, and STTC are timescale dependent, the in silico manipulated data are based on the experimental data (see section 2.3) in order to obtain realistic timescales. In all, 10 recordings from 5 independent networks ($N = 5$) were used (5 without and 5 with 10 μM BIC). Each recording had a length of 300 s and up to 60 active electrodes. The following procedures were applied for every active electrode (active if at least 6 spikes per minute; see section 2.3.2) with X being the spike train of the original electrode and Y being the manipulated spike train:

1. *Added spikes.* Spike train Y was generated by copying spike train X and adding N_{add} spikes to Y with temporal positions randomly assigned in the range of $(0, 300]$ s. In case of identical spike times, new random spike times were generated until all spike times were unique. Depending on the manipulation level the number of added spikes was

$$N_{add} = L \cdot 0.1 \cdot N_X, \tag{2.1}$$

   with N_X being the number of spikes in spike train X and L being the manipulation level in the range of $L = [0, 0.1, 0.2 \ldots 1]$ ($L = 0$: No manipulation, $L = 1$: 10% random spikes were added). For each L, 40 independent random manipulations ($n_{manipulated} = 40$) were performed (see Figure 1b(1) for example spike trains).
2. *Deleted spikes.* Spike train Y was generated by copying spike train X and deleting N_{delete} randomly selected spikes from Y. Depending on

[1] http://wwwold.fi.isc.cnr.it/users/thomas.kreuz/Source-Code/cSPIKE.html.
[2] https://github.com/biomemsLAB/Spike-Contrast.
[3] https://de.mathworks.com/matlabcentral/fileexchange/28694-mutual-information.
[4] http://neuralensemble.org/elephant/.
[5] https://github.com/biomemsLAB/SynchronyMeasures-Robustness.

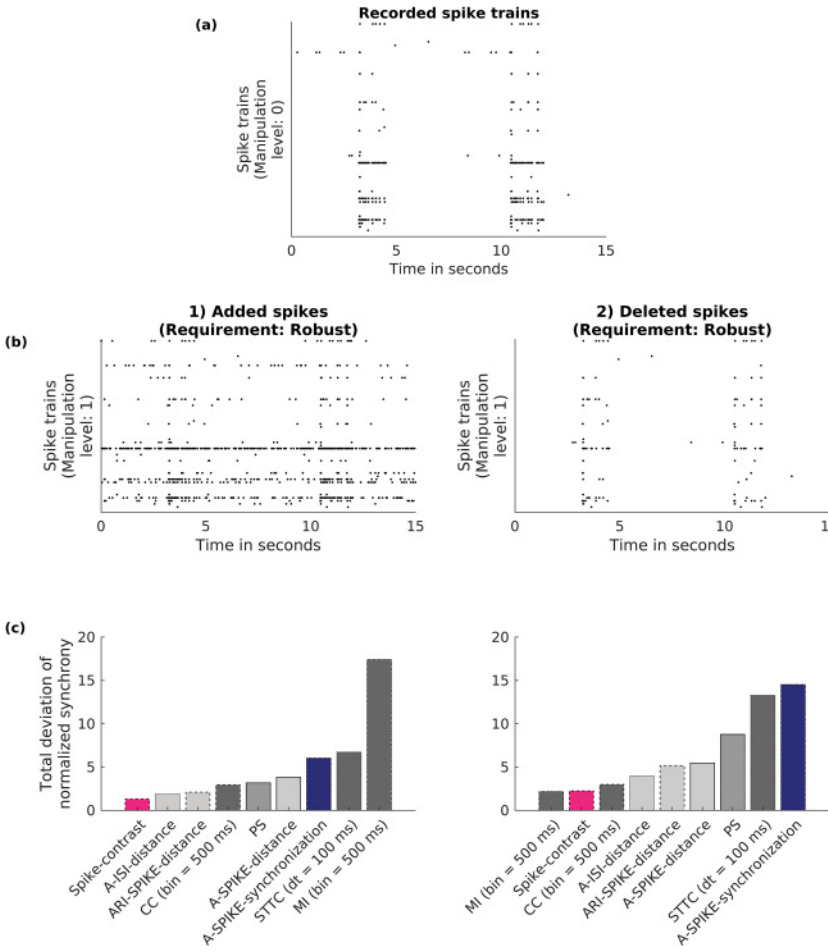

Figure 1: Comparison of different synchrony measures regarding their robustness to erroneous spike trains. (a) Spike trains recorded from 60 electrodes with 10 μM BIC. Each line represents the spike train of one electrode (only first 15 s of 300 s are displayed). (b) Same as panel a but with maximum manipulation level applied (left: simulation of false-positive spikes; right: simulation of false-negative spikes). Ten different recordings were used to generate the in silico manipulated data (for details, see section 2.2). (c) Sum of synchrony deviation over all manipulation levels (denoted as total deviation of the normalized synchrony, TDNS; see equation 2.5). The lower the TDNS value of a synchrony measure, the more robust it is to spike train manipulation.

the manipulation level, the number of deleted spikes was

$$N_{delete} = L \cdot 0.9 \cdot N_X, \tag{2.2}$$

where N_X is the number of spikes in spike train X and L is the manipulation level in the range of $L = [0, 0.1, 0.2, \ldots 1]$ ($L = 0$: No manipulation, $L = 1$: 90% of all spikes were deleted). Note that the maximum range was restricted to 90% of N_X as some of the tested synchrony measures were not defined for empty spike trains. For each L, 40 independent random manipulations ($n_{manipulated} = 40$) were performed (see Figure 1b(2) for example spike trains).

A single synchrony value was then calculated for every recording ($N = 10$) and every random manipulation ($n_{manipulated} = 40$). Overall, for every manipulation level, 400 synchrony values were calculated per synchrony measure.

Because some of the synchrony measures differ in terms of their minimum value for Poisson spike trains with equal rate (e.g., 0.295 for SPIKE-distance and 0.5 for ISI-distance (Kreuz et al., 2013)), they could not be compared directly. Therefore, synchrony values of each measure were rescaled to their lowest possible synchrony value defined as synchrony of a data set made of Poisson spike trains $Y_{L,random}$ at the manipulation level L. The number of spikes in $Y_{L,random}$ was equal to the number of spikes in Y_L (being the manipulated spike train Y at the manipulation level L) to account for the spike rate dependence of some synchrony measures, as reported in Cutts and Eglen (2014). The scaling was done with

$$s'_L = \frac{s_L - \bar{s}_{L,random}}{1 - \bar{s}_{L,random}}, \tag{2.3}$$

where s_L is the synchrony value at a manipulation level L, $\bar{s}_{L,random}$ is the mean synchrony value of the data set consisting of Poisson spike trains $Y_{L,random}$, and value 1, representing the largest possible synchrony value (all synchrony measures were able to yield 1 for identical spike trains). As 10 different recordings with different synchrony level were used, all synchrony values were normalized, allowing us to calculate the mean over all recordings and all random realizations. The normalization was done with

$$s''_L = \frac{s'_L}{s'_{L=0}}, \tag{2.4}$$

where $s'_{L=0}$ is the synchrony of the orginal spike train (manipulation level $L = 0$) and s''_L is the normalized synchrony value. All normalized synchrony values of all recordings and all random realizations taken together are denoted as $s''_{L,all}$. In order to ease the comparison among the different

synchrony measures, the total deviation of the normalized synchrony (TDNS) over the manipulation level was calculated as

$$TDNS = \sum_{L=0}^{1} std(s''_{L,all}), \tag{2.5}$$

where $std()$ is the standard deviation. The lower the TDNS, the more robust the synchrony measure against the spike train manipulation procedure.

2.3 Experimental Data.

2.3.1 Cell Culture and Electrophysiological Recordings. Experimental data used for this study were recorded from primary cortical neurons (Lonza Ltd., Basel, Switzerland) harvested from embryonic rats (E18 and E19). Cell cultivation followed a modified protocol based on Otto, Goertz, Fleischer, and Siebler (2003). Briefly, vials containing 4×10^6 cells were stored in liquid nitrogen at -196°C. After thawing, cells were diluted drop-wise with prewarmed cell culture medium and seeded at a density of 5000 cells/mm^2 onto Poly-D-Lysine and Laminin coated (Sigma Aldrich, St. Louis, U.S.A.) microelectrode arrays (60MEA200/30iR-Ti, Multichannel Systems MCS GmbH, Reutlingen, Germany). Twice a week, half of the medium was replaced with fresh, prewarmed medium.

Neuronal signals were recorded extracellularly at a sampling rate of 10 kHz outside the incubator at -37°C employing a temperature-controller (Multichannel Systems MCS). For drug-induced increase of network synchronization, BIC (Sigma Aldrich Co.) was applied to the neuronal cell culture after 21 days in vitro (div) at a concentration of 10 μM. BIC is a competitive antagonist of the $GABA_A$ receptor. Since it blocks the inhibitory function of $GABA_A$ receptors, its application yields an increased incidence of synchronized burst events (Jungblut, Knoll, Thielemann, & Pottek, 2009; see Figures 2b and 2c). Neuronal activity was recorded for 5 minutes before and 5 minutes during the application of BIC.

2.3.2 Spike Detection. Raw data were stored for offline spike detection with DrCell, a custom-made Matlab software tool, developed by Nick et al. (2013). After applying a high-pass filter with a cutoff frequency of 50 Hz, spikes were separated from noise using a threshold-based algorithm, with a threshold calculated by multiplying the standard deviation of the noise by a factor of 5 (or, more precisely, -5, as only negative spikes were used for analysis). As soon as the raw signal underran the threshold, the time of the minimum voltage value was defined as a spike time stamp (see Figure 2a). Additionally, in order to alter the level of false-positive and false-negative spikes, spike detection was conducted using threshold factors of 4, 6, and 7. For subsequent spike train analysis, only electrodes with more than 5 spikes

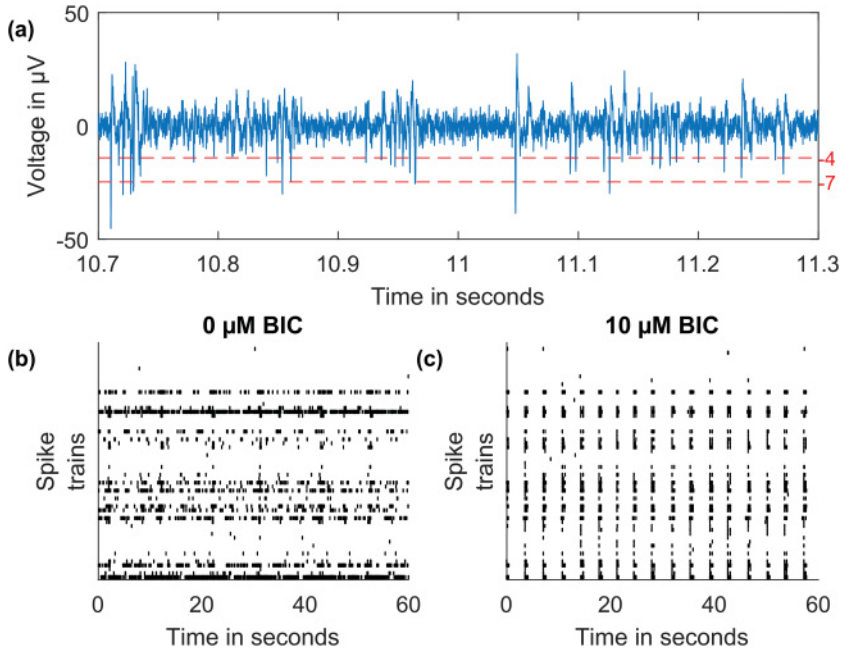

Figure 2: Exemplary illustration of the experimental data. (a) Signal recorded from one MEA electrode (50 Hz high-pass filtered). Thresholds are displayed for the lowest (4) and highest (7) threshold factors used for spike detection. The higher the threshold factor, the fewer spikes are detected. (b) Rasterplot of the spontaneous activity of one MEA chip without BIC (only first 60 s of 300 s are shown). (c) Same as panel b but with 10 μM BIC. Spontaneous activity was recorded with a 60 electrode MEA chip at 23 div. Compared to the native state, the administration of 10 μM BIC increased the level of synchrony.

per minute were considered active and used for analysis (Novellino et al., 2011).

2.3.3 Statistical Analysis. Since it is known that BIC causes an increase of network synchrony in cortical neurons in vitro (Sokal et al., 2000; Chiappalone et al., 2007; Eisenman et al., 2015), a one-tailed statistical test was applied. More specifically, a paired t-test was applied under the null hypothesis that BIC does not increase synchrony. The lower the p-value, the lower the probability that there is no synchrony change and, hence, the better the synchrony measure's sensitivity to BIC.

2.4 Parameter Choice. As the synchrony measures CC, MI, and STTC depend on a timescale parameter that directly influences the synchrony

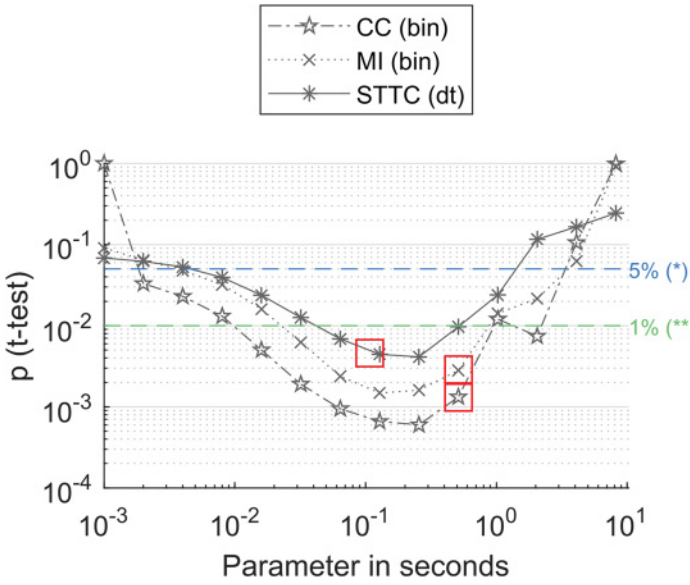

Figure 3: Influence of the parameter choice on the statistical significance of the experimental data. The synchrony measures CC, MI, and STTC depend on a parameter that has to be chosen by the user. For each synchrony measure, the experimental data described in section 2.3 were analyzed using different parameter values. After that, a *t*-test was applied to the data with the null hypothesis that synchrony values of the data with BIC are lower than or equal to synchrony values of the data without BIC. In this work, a bin size of 500 ms was used for CC and a *dt* of 100 ms for STTC (red squares), values that were suggested in their original publications (Selinger et al., 2004; Cutts & Eglen, 2014). For MI, the same bin size as for CC was used due to the identical binning procedure.

definition, an appropriate parameter value had to be chosen. Therefore, we analyzed the experimental BIC data using different parameter values and conducted a statistical hypothesis test. The lower the *p*-value, the higher the probability that an increase in synchrony occurred. Parameter values that lead to low *p*-values are therefore desirable (given that BIC results in increased level of synchrony). CC, proposed by Selinger et al. (2004), chose a bin size of 500 ms, which also gave reasonable low *p*-values in our analysis (see Figure 3). Even if smaller bin sizes yielded lower *p*-values in our data, we stuck to the predefined 500 ms. For MI, we also chose a bin size of 500 ms as for smaller bin sizes, the *p*-value improved only slightly. The parameter *dt* of STTC was set to 100 ms according to the original publication from Cutts and Eglen (2014). Note that in our cortical data, a larger *dt* value would improve the *p*-value only slightly.

3 Results

3.1 Comparison of Synchrony Measures for *in Silico* Manipulated Data. For added spikes, the robustness of measures was studied by randomly adding false-positive spikes to the basic signals. For a robust synchrony measure, low sensitivity to false-positive spikes is desirable, as such noise may falsify the results. As displayed in Figure 1c(left). Spike-contrast was most robust to false-positive spikes indicated by the small TDNS value of around 1, closely followed by A-ISI-distance and ARI-SPIKE-distance. MI showed by far the largest synchrony deviation indicated by a TDNS value of around 17.

For deleted spikes, a similar picture occurs after increasingly deleting spikes in order to simulate false-negative spikes, as robustness to false-negative spikes was required. In Figure 1c(right), the results of synchrony measure dependency to false-negative spikes are shown. Here, MI and Spike-contrast were most robust to false-negative spikes yielding the smallest TDNS value of around 2. STTC and A-SPIKE-synchronization showed the largest TDNS value of around 14.

3.2 Comparison of Synchrony Measures for Experimental Data. In addition to the evaluation with in silico manipulated data, all synchrony measures were applied to experimental data recorded from cortical neurons by MEA chips with and without the application of 10 μM BIC. Figure 4a shows the absolute synchrony values for each synchrony measure and for all different cell cultures ($N = 5$), before and after the application of BIC. Generally all measures showed a significant synchrony increase due to the BIC application with p-values of 5% and below, where A-SPIKE-synchronization, A-ISI-distance, and A-SPIKE-distance failed to reach the high significance level of 1%.

In order to alter the level of false-positive and false-negative spikes in the experimental data, different spike detection threshold factors (4 to 7) were applied, where low thresholds are likely to correspond to additional false spikes (false positive) and high thresholds to missed spikes (false negative). Increasing the threshold factor is comparable to deleting spikes from the spike train, as already done in the in silico manipulated data evaluation (see section 3.1). For the in silico manipulated data, the synchrony measures STTC and A-SPIKE-synchronization were most sensitive to deleted spikes. This behavior was also evident within the experimental data (see Figure 5). As the spike detection threshold factor increased, STTC and A-SPIKE-synchronization lose their statistical significance (above 5% level), while all others remained stable, indicating statistical significance (below 5% level). Spike-contrast yielded the highest statistical significance across all tested threshold factors and was the only measure that still indicated a statistical significance (at 5% level) at the smallest threshold factor of 4, where a high level of noise spikes is assumable.

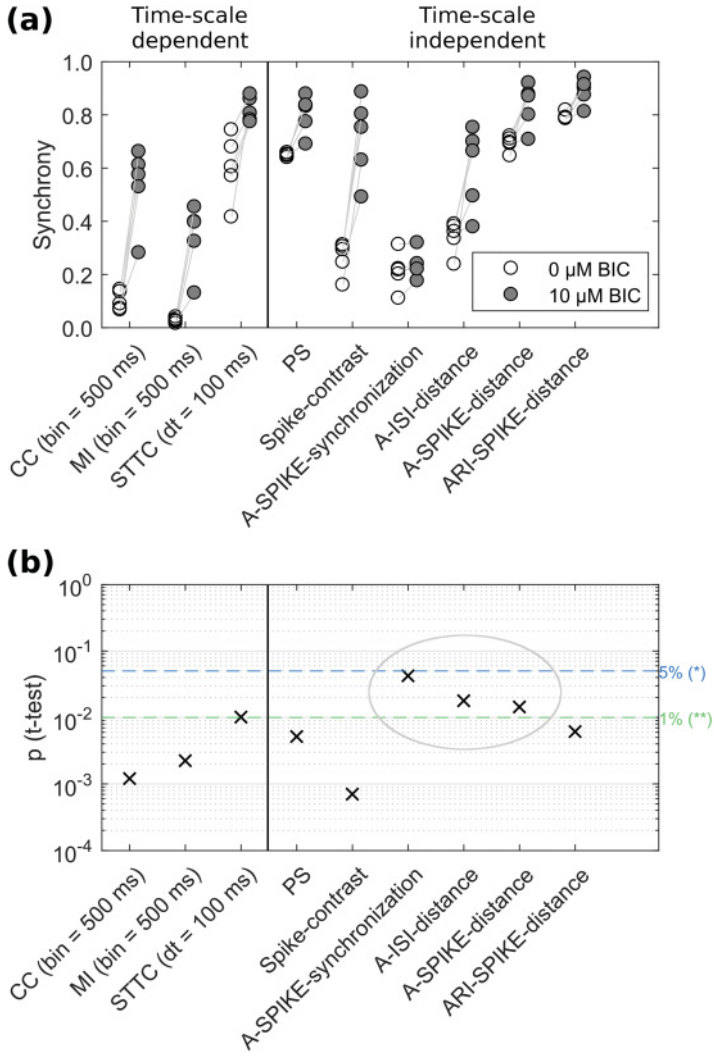

Figure 4: Results of the application of different timescale-dependent and timescale-independent synchrony measures to a set of experimental data. Experimental data were recorded from cortical cell cultures on MEA chips ($N = 5$) in the absence and presence of 10 μM BIC. (a) Absolute synchrony values of each synchrony measure for data without BIC (white circles) and with BIC (gray circles). (b) P-values for each synchrony measure from a one-tailed paired t-test assuming an increase in synchrony. The lower the p-value, the better the synchrony measure's ability to capture the effect of BIC. The gray ellipse marks synchrony measures that were not able to indicate high significant effects below p-values of 1%. Spike detection threshold factor was 5.

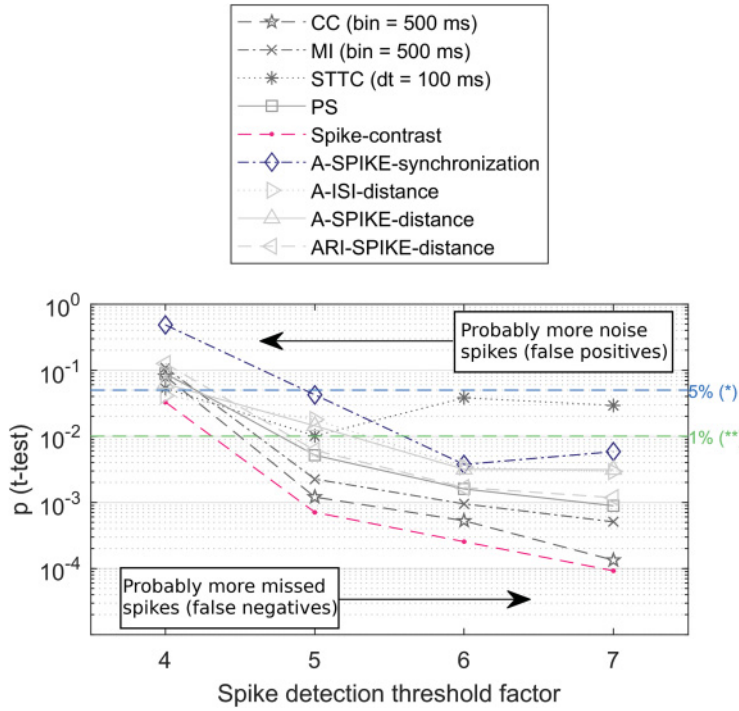

Figure 5: Influence of the spike detection threshold on the statistical significance of the experimental data. Synchrony and the statistical significance of the experimental data were analyzed as in Figure 4, applying different thresholds to detect spikes from the recorded signals. The higher the spike detection threshold factor, the less noise was detected, but also more real spikes were missed. The lower the *p*-value, the better the synchrony measure's ability to capture the effect of BIC.

4 Discussion and Conclusion

In this work, we compared different spike train synchrony measures regarding their robustness to false-positive and false-negative spikes in epileptiform signals. Such robustness is particularly relevant for experimental data with error-prone spike detection, especially at low signal-to-noise ratios. Representative synchrony measures were chosen from different categories such as timescale-dependent (CC, MI, STTC) or timescale-independent (Spike-contrast, PS, A-SPIKE-synchronization, A-ISI-distance, A-SPIKE-distance, ARI-SPIKE-distance). In order to perform a comparison, we proposed a procedure based on a set of in silico manipulated spike trains with defined manipulation of features. Two data

sets were generated based on experimental data by adding spikes, representing noise (false positive), and deleting spikes, representing missed spikes (false negative). Synchrony of the experimental data was increased by applying BIC to cortical in vitro networks. The code and data used in this work are publicly available (see section 2.1).

For the in silico manipulated data, the results showed that Spike-contrast was the most robust to added spikes and very robust to deleted spikes. All other measures showed comparable high robustness for added or deleted spikes but not for both cases. Furthermore, CC, MI, and Spike-contrast work with binned spike trains, which explains their robustness to deleted spikes as long as bursts (many spikes occurring within a small time period) are still present in the data (see Figure 1b(2)). A binned spike train will almost not change if only some spikes are deleted from a burst and if the bin size and burst duration are similar. As Spike-contrast automatically adapts its bin size to the data, it is preferable to CC and MI for exploratory studies, where the timescale is not known beforehand.

For the experimental data, all synchrony measures captured the synchrony increase mediated by BIC in a statistically significant way (below a p-value of 5%). However, there were differences in performance as the synchrony measures CC, MI, PS, Spike-contrast, and ARI-SPIKE-distance yielded values leading to a high statistical significance below p-values of 1%. Note that for CC, the proposed bin size of 500 ms was used, but smaller bin sizes of around 300 ms would have overperformed Spike-contrast (see Figure 3). Referring to our assumption that the lower the p-value, the better the synchrony measure (defined in section 2.3), it must be taken into account that this assumption is controversial since the actual synchrony increase (ground truth) is not known for the experimental data. Thus, a synchrony measure that overestimates the synchrony increase mediated by BIC would incorrectly lead to a low p-value.

For small sample sizes, as in our experiment ($N = 5$), parameter-free statistics like the Wilcoxon signed-rank test are generally used to avoid assumptions about population distribution. Application of the Wilcoxon signed-rank test to our data yielded almost identical p-values for all synchrony measures (data not shown). In contrast, the t-test used in this work resulted in different p-values for each synchrony measure. So it also depends on the choice of statistical test whether the choice of synchrony measures affects the final results.

Considering the results of the in silico manipulated data, the measures CC, MI, Spike-contrast, and ARI-SPIKE-distance were most robust to deleted spikes (false-negative spikes). These synchrony measures also showed the best performance in the experimental data, which suggests that robustness to false-negative spikes correlates with the ability to quantify synchrony changes in experimental data. If so, it would also imply that the experimental data used in this work were more affected by false-negative spikes than by false-positive spikes. In other words, more

spikes were missed than noise was misinterpreted as spikes. This behavior could be used to draw conclusions about the quality of an experimental spike train from the rank of the p-values of different synchrony measures.

As already mentioned, there were some synchrony measures whose results of the in silico manipulated data and experimental data did not correlate. This suggests that robustness to false-positive or false-negative spikes is not the only factor to effectively capture synchrony changes in experimental data. Factors like robustness to temporal nonstationarity of the recording could also be different among the synchrony measures. For instance, PS, A-SPIKE-distance, ARI-SPIKE-distance, A-ISI-distance, and A-SPIKE-synchronization are more adaptive to changes in timescales inside a spike train as they dynamically define their timescales considering nearby spikes. In contrast, CC, MI, STTC, and Spike-contrast use equally spaced timescales along the entire spike train duration.

Overall, for our specific data set, Spike-contrast was the only timescale-independent measure being robust to noise (false-positive spikes) as well as missed spikes (false-negative spikes). This desirable performance was confirmed by the ability of the Spike-contrast measure to detect biochemically induced synchrony with high significance, even for different spike detection threshold factors. It should be mentioned that the measures A-SPIKE-synchronization, A-ISI-distance, A-SPIKE-distance, and ARI-SPIKE-distance are able to produce a synchrony profile over time, which complements the synchrony profile over the timescale of Spike-contrast.

We suggest including the Spike-contrast synchrony measure in synchrony studies of epileptiform experimental neuronal data sets in addition to established synchrony measures.

Appendix: Synchrony Measure Description

A.1 Mutual Information. MI measures how two random variables X and Y are related (Cover & Thomas, 2012) and is based on the concept of entropy, a fundamental concept in information theory (Shannon & Weaver, 1948; Cover & Thomas, 2012). The Shannon entropy (Cover & Thomas, 2012) of a random variable X is defined as

$$H(X) = -\sum_i p_x(i) \log(p_x(i)), \tag{A.1}$$

where $p_x(i) = P(X = i)$ and the log function is taken to base 2 (see Figure 6a for an example calculation). $H(X)$ measures the uncertainty about a random variable X. The conditional entropy quantifies the information necessary to describe the random variable Y given that the information about X is known

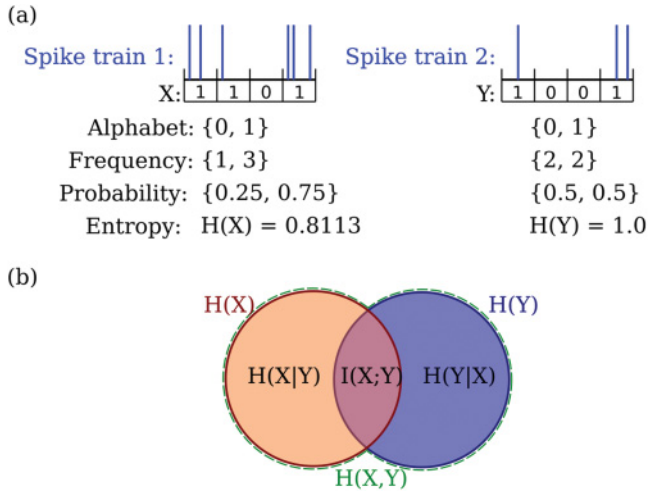

Figure 6: Example entropy calculation of two spike trains and illustration of the mutual information (MI) measure. (a) Two different spike trains are binned in a binary way, resulting in X and Y. Each value is considered a character building the alphabet of the signal. The probability of each character is obtained by dividing its incidence by the length of the signal. The entropy of each signal (H(X), H(Y)) is calculated using equation A.1 with the probabilities given above. (b) Visualization of the mutual information I(X;Y) using the joint entropy H(X,Y), the entropies H(X), H(Y), and conditional entropies H(X|Y), H(Y|X) calculated in equation A.4. The mutual information value I(X;Y) increases with increasing synchrony between signal X and Y.

(Cover & Thomas, 2012). Formally, it is defined by

$$\begin{aligned} H(Y|X) &\equiv \sum_{x\in X} p(x)\, H(Y|X=x) \\ &= \sum_{x\in X}\left(p(x)\sum_{y\in Y} p(y|x)\,\log\,\frac{1}{p(y|x)}\right) \\ &= -\sum_{x\in X}\sum_{y\in Y} p(x,y)\,\log\,p(y|x) \\ &= -\sum_{x\in X, y\in Y} p(x,y)\log\,p(y|x) \\ &= \sum_{x\in X, y\in Y} p(x,y)\log\frac{p(x)}{p(x,y)}. \end{aligned} \tag{A.2}$$

MI is defined as

$$I(X;Y) = \sum_{y \in Y} \sum_{x \in X} p(x,y) \log \left(\frac{p(x,y)}{p(x)\, p(y)} \right). \tag{A.3}$$

Additionally, the MI can be expressed in terms of the entropy and the conditional entropy of random variables X and Y as

$$\begin{aligned} I(X;Y) &= H(X) - H(X|Y) \\ &= H(Y) - H(Y|X) \\ &= H(X) + H(Y) - H(X,Y) \\ &= H(X,Y) - H(X|Y) - H(Y|X). \end{aligned} \tag{A.4}$$

Aside from the analytic expressions, it is possible to interpret those quantities graphically, as depicted in Figure 6b. MI is more general than the correlation coefficient and quantifies how the joint distribution $p(x, y)$ is similar to the products of marginal distributions $p(x)p(y)$ (Cover & Thomas, 2012). Compared to the cross-correlation measure, mutual information also captures nonlinear dependencies.

For comparison, the value of mutual information needs to be normalized. Many possible approaches have been proposed (Cover & Thomas, 2012), such as

$$M(X;Y) = \frac{I(X;Y)}{\min\left[H(X), H(Y)\right]}, \tag{A.5}$$

because $I(X;Y) \leq \min\left[H(X), H(Y)\right]$ and, consequently, $0 \leq M(X;Y) \leq 1$. This formulation has been used before in the context of neuronal signal analysis (Bettencourt, Stephens, Ham, & Gross, 2007; Bettencourt, Gintautas, & Ham, 2008; Ham et al., 2010). Another possible normalization is the so-called symmetric uncertainty (Witten & Frank, 2000), defined as

$$M^*(X;Y) = 2\frac{I(X;Y)}{H(X) + H(Y)}, \tag{A.6}$$

where $0 \leq M^*(X;Y) \leq 1$. In this work the latter normalization was used as it performed better than the first one when applied to the experimental data (data not shown).

In order to estimate the MI between two spike trains, both spike trains were transformed into binary binned signals. A spike train i is binned as

$$x_i(t) = \begin{cases} 1, & \text{if spike train } i \text{ shows at least one spike in time interval } t \text{ to } t + \Delta t \\ 0, & \text{if spike train } i \text{ shows no spike in time interval } t \text{ to } t + \Delta t \end{cases}, \tag{A.7}$$

using a bin size $\Delta t = 500$ ms and $t = 0\Delta t, 1\Delta t, 2\Delta t, \ldots$ (also see Figure 6a). The choice of the bin size of 500 ms is justified in section 2.4).

A.2 Phase Synchronization. Since synchronization processes are related to rhythm adjustment, it is natural to introduce the concept of phase of an oscillator, a quantity that increases by 2π within an oscillation cycle and determines unambiguously the state of a periodic oscillator (Pikovsky, Rosenblum, & Kurths, 2003). For instance, consider a harmonic oscillator described by the variable $x(t) = A\sin(\omega_0 t + \phi_0)$. In this case, ω_0 denotes the angular frequency, which is related to the oscillation period $\omega_0 = 2\pi/T$, A is the amplitude of oscillation, and the quantity $\phi(t) = \omega_0 t + \phi_0$ is the phase of this oscillator. Two or more oscillators are synchronized when they present the same phase evolution (Pikovsky et al., 2003).

The measurement of the synchronization level of self-sustained oscillators can be done by considering the phases as rotating points in the unit cycle of the complex plane (Pikovsky et al., 2003; Strogatz, 2000). If an oscillator has a phase $\phi(t)$, its trajectory in the complex plane is described by the vector $e^{i\phi(t)}$. For instance, if two oscillators have phases $\phi_1(t) = \phi_2(t) = \phi(t)$, they will have the same trajectory in the complex plane, and thus the modulus of the resultant vector will be $|e^{i\phi_1(t)} + e^{i\phi_2(t)}|/2 = 1$, meaning that the oscillators are perfectly synchronized. Now suppose a population of N interacting phase oscillators whose phases are described by the variable $\phi_i(t)$, $i = 1, \ldots, N$. The synchronization order parameter is defined as (Strogatz, 2000)

$$re^{i\psi(t)} = \frac{1}{N}\sum_{j=1}^{N} e^{i\phi_j(t)}, \tag{A.8}$$

where $\psi(t)$ is the average phase of the system at time t. When $r \approx 0$, the phases are distributed uniformly over $[0, 2\pi]$ corresponding to the asynchronous state. When $r \approx 1$ the phases rotate together, corresponding to a fully synchronized state (see Figure 7).

Neurons can also be considered as self-sustained oscillators (Arenas, Díaz-Guilera, Kurths, Moreno, & Zhou, 2008) and are often modeled as integrate-and-fire oscillators, where the rhythmic quantity is the rate at which spikes are fired. The synchronization process in this case is the adjustment of the spiking patterns: if two interacting integrate-and-fire oscillators discharge their spikes jointly, they are synchronized. Therefore, in order to

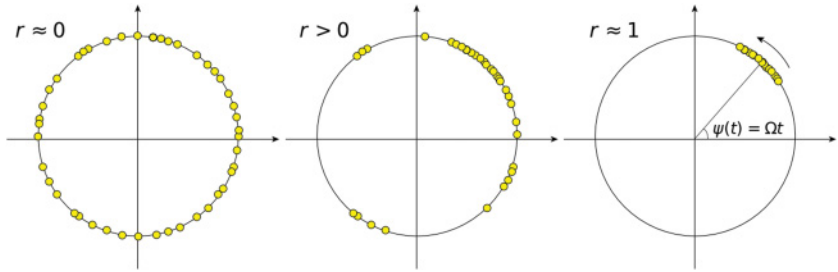

Figure 7: Example for distribution of phase vectors $e^{i\phi(t)}$ in complex plane. (a) Randomly distributed phase vectors over $[0, 2\pi]$, implying $r \approx 0$; in other words, the oscillators are completely asynchronous. (b) Regime of partial synchronization; phase vectors of some oscillators are grouped in a synchronous cluster equivalent to $r > 0$. (c) Strongly synchronized state, where all oscillators group into a single synchronous cluster rotating with average frequency Ω; thus, $r \approx 1$.

quantify the synchronization between interacting integrate-and-fire oscillators, the phases associated with the respective spike signals have to be defined.

The time series recorded by an electrode can be considered as a sequence of point events taking place at time t_k, with $k = 1, 2, \ldots, N_{\text{spikes}}$. The time interval between two spikes can be treated as a complete cycle. In this case, the phase increase during this time interval is exactly 2π. Hence, the values of $\phi(t_k) = 2\pi k$ are assigned to the times t_k, and for an arbitrary instant of time ($t_k < t < t_{k+1}$), the phase is considered a linear interpolation between these values (Pikovsky et al., 2003; Neiman, Silchenko, Anishchenko, & Schimansky-Geier, 1998; Pikovsky et al., 1997; Tass et al., 1998; Hu & Zhou, 2000), as

$$\phi(t) = 2\pi \frac{t - \tau_k}{\tau_{k+1} - \tau_k} + 2\pi k. \tag{A.9}$$

This method can be applied to any process containing time series of spikes, and it is widely used in the study of synchronization in neuronal dynamics (Pikovsky et al., 2003). Figure 8 exemplifies the calculation of phases $\phi(t)$ of two spike signals and their respective sum of the phase vectors $e^{i\phi(t)}$ in the complex plane.

For a system composed of N oscillators, the instant phase synchronization is quantified by the order parameter defined in equation A.8. However, to quantify the level of synchronization of the neurons, we consider the average over the recorded time,

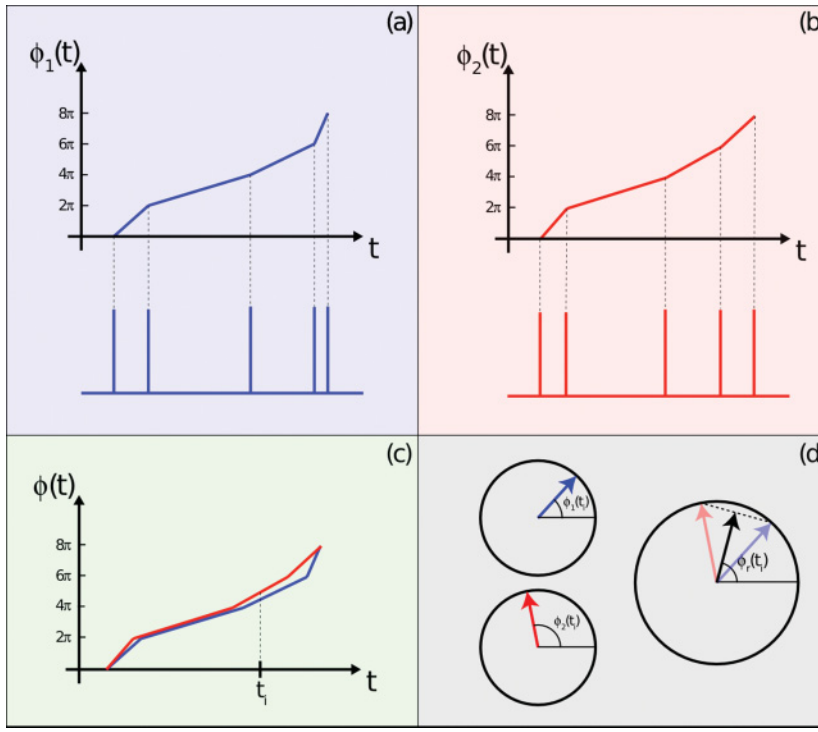

Figure 8: Example of phase vector construction. (a) $\phi_1(t)$ and (b) $\phi_2(t)$ are calculated using the respective spike signals according to equation A.9. (c) Superposition of temporal evolution of phases and (d) phase vectors $e^{i\phi_1(t_i)}$, $e^{i\phi_2(t_i)}$ as well as the resultant vector at time $t = t_i$, $r \cdot e^{i\phi_r(t_i)} = (e^{i\phi_1(t_i)} + e^{i\phi_2(t_i)})/2$.

$$\bar{r} = \left\langle \left| \frac{1}{N} \sum_{j=1}^{N} e^{i\phi_j(t)} \right| \right\rangle_t , \tag{A.10}$$

where $\langle \cdots \rangle_t$ stands for the temporal average and N stands for the number of electrodes used to compute the order parameter.

Acknowledgments

F.A.R. acknowledges CNPq (grant 305940/2010-4), Fapesp (grants 2012/51301-8 and 2013/26416-9), and NAP eScience-PRP-USP for financial support. L.F.C. thanks CNPq (grant 307085/2018-0) and FAPESP (grant 15/22308-2) for sponsorship. G.F.A. acknowledges FAPESP (grant 2012/25219-2). T.P. acknowledges FAPESP (grant 2016/23827-6). C.C.H.

acknowledge FAPESP (grant 18/09125-4). C.T. and M.C. acknowledges Bayerisches Staatsministerium für Bildung und Kultus, Wissenschaft und Kunst for financial support in the frame of ZEWIS, BAYLAT, the BMBF (grant 03FH061PX3), and the INeuTox (grant 13FH516IX6). C.N. acknowledges support from the Studienstiftung des Deutschen Volkes.

Author Contributions

M.C.: Conception, design, generation, and analysis of in silico manipulated data. Application of the synchrony measures STTC, Spike-contrast, A-SPIKE-synchronization, A-ISI-distance, A-SPIKE-distance, and ARI-SPIKE-distance to experimental data. Statistical tests and spike detection with varying thresholds. Preparation of Figures 1 to 6. Draft of the manuscript. R.B.: Initial conception and design of synchrony measure comparison using experimental data. C.N.: Initial conception and design of synchrony measure comparison using experimental data. Performed cell experiments and spike detection of raw data. G.F.A.: Implementation and application of the synchrony measure MI to experimental data and MI description in the appendix. T.P.: Implementation and application of the synchrony measure PS to experimental data and PS description in the appendix. Preparation of Figures 7 and 8. C.C.H.: Implementation and application of the synchrony measures CC to the experimental data. L.F.C.: Helped in the initial conception, discussions, and revision. F.A.R.: Conception and design of research. C.T.: Conception and design of research. All: Interpreted and discussed results of experiments.

References

Andrzejak, R. G., Mormann, F., & Kreuz, T. (2014). Detecting determinism from point processes. *Physical Review E*, *90*(6), 062906.

Arenas, A., Díaz-Guilera, A., Kurths, J., Moreno, Y., & Zhou, C. (2008). Synchronization in complex networks. *Physics Reports*, *469*(3), 93–153.

Arnulfo, G., Canessa, A., Steigerwald, F., Pozzi, N. G., Volkmann, J., Massobrio, P., . . . Isaias, I. U. (2015). Characterization of the spiking and bursting activity of the subthalamic nucleus in patients with Parkinson's disease. In *Proceedings of the 2015 International Conference on Advances in Biomedical Engineering* (pp. 107–110). Piscataway, NJ: IEEE.

Bettencourt, L. M. A., Gintautas, V., & Ham, M. I. (2008). Identification of functional information subgraphs in complex networks. *Phys. Rev. Lett.*, *100*, 238701.

Bettencourt, L., Stephens, G., Ham, M., & Gross, G. (2007). Functional structure of cortical neuronal networks grown in vitro. *Physical Review*, *E 75*(2), 021915.

Chiappalone, M., Bove, M., Vato, A., Tedesco, M., & Martinoia, S. (2006). Dissociated cortical networks show spontaneously correlated activity patterns during in vitro development. *Brain Research*, *1093*(1), 41–53.

Chiappalone, M., Vato, A., Berdondini, L., Koudelka-Hep, M., & Martinoia, S. (2007). Network dynamics and synchronous activity in cultured cortical neurons. *International Journal of Neural Systems*, *17*(2), 87–103.

Ciba, M., Isomura, T., Jimbo, Y., Bahmer, A., & Thielemann, C. (2018). Spike-contrast: A novel time scale independent and multivariate measure of spike train synchrony. *Journal of Neuroscience Methods*, *293* (Suppl. C), 136–143.

Cover, T. M., & Thomas, J. A. (2012). *Elements of information theory*. Hoboken, NJ: Wiley.

Cutts, C. S., & Eglen, S. J. (2014). Detecting pairwise correlations in spike trains: An objective comparison of methods and application to the study of retinal waves. *Journal of Neuroscience*, *34*(43), 14288–14303.

Dura-Bernal, S., Li, K., Neymotin, S. A., Francis, J. T., Principe, J. C., & Lytton, W. W. (2016). Restoring behavior via inverse neurocontroller in a lesioned cortical spiking model driving a virtual arm. *Frontiers in Neuroscience*, *10*.

Eisenman, L. N., Emnett, C. M., Mohan, J., Zorumski, C. F., & Mennerick, S. (2015). Quantification of bursting and synchrony in cultured hippocampal neurons. *Journal of Neurophysiology*, *114*(2), 1059–1071.

Engel, A. K., Fries, P., & Singer, W. (2001). Dynamic predictions: Oscillations and synchrony in top-down processing. *Nature Reviews Neuroscience*, *2*(10), 704–716.

Espinal, A., Rostro-Gonzalez, H., Carpio, M., Guerra-Hernandez, E. I., Ornelas-Rodriguez, M., Puga-Soberanes, H., . . . Melin, P. (2016). Quadrupedal robot locomotion: A biologically inspired approach and its hardware implementation. *Computational Intelligence and Neuroscience*, *2016*, 1–13.

Fisher, R. S., Boas, W. v. E., Blume, W., Elger, C., Genton, P., Lee, P., & Engel, J. (2005). Epileptic seizures and epilepsy: Definitions proposed by the International League against Epilepsy (ILAE) and the International Bureau for Epilepsy (IBE). *Epilepsia*, *46*(4), 470–472.

Flachs, D., & Ciba, M. (2016). Cell-based sensor chip for neurotoxicity measurements in drinking water. *Lékař a technika—Clinician and Technology*, *46*(2), 46–50.

Ham, M. I., Gintautas, V., Rodriguez, M. a., Bennett, R. a., Maria, C. L. S., & Bettencourt, L. M. a. (2010). Density-dependence of functional development in spiking cortical networks grown in vitro. *Biological Cybernetics*, *102*(1), 71–80.

Hu, B., & Zhou, C. (2000). Phase synchronization in coupled nonidentical excitable systems and array-enhanced coherence resonance. *Phys. Rev. E*, *61*, R1001–R1004.

Jungblut, M., Knoll, W., Thielemann, C., & Pottek, M. (2009). Triangular neuronal networks on microelectrode arrays: An approach to improve the properties of low-density networks for extracellular recording. *Biomedical Microdevices*, *11*(6), 1269–1278.

Kreuz, T., Chicharro, D., Greschner, M., & Andrzejak, R. G. (2011). Time-resolved and time-scale adaptive measures of spike train synchrony. *Journal of Neuroscience Methods*, *195*(1), 92–106.

Kreuz, T., Chicharro, D., Houghton, C., Andrzejak, R. G., & Mormann, F. (2013). Monitoring spike train synchrony. *Journal of Neurophysiology*, *109*(5), 1457–1472.

Kreuz, T., Haas, J. S., Morelli, A., Abarbanel, H. D., & Politi, A. (2007). Measuring spike train synchrony. *Journal of Neuroscience Methods*, *165*(1), 151–161.

Kreuz, T., Mulansky, M., & Bozanic, N. (2015). Spiky: A graphical user interface for monitoring spike train synchrony. *Journal of Neurophysiology*, *113*(9), 3432–3445.

Li, W., Doyon, W. M., & Dani, J. A. (2011). Acute in vivo nicotine administration enhances synchrony among dopamine neurons. *Biochemical Pharmacology*, *82*(8), 977–983.

Lieb, F., Stark, H.-G., & Thielemann, C. (2017). A stationary wavelet transform and a time-frequency based spike detection algorithm for extracellular recorded data. *Journal of Neural Engineering*, *14*(3), 036013.

Neiman, A., Silchenko, A., Anishchenko, V., & Schimansky-Geier, L. (1998). Stochastic resonance: Noise-enhanced phase coherence. *Phys. Rev. E*, *58*, 7118–7125.

Nick, C., Goldhammer, M., Bestel, R., Steger, F., Daus, A., & Thielemann, C. (2013). Drcell a software tool for the analysis of cell signals recorded with extracellular microelectrodes. *Signal Processing: An International Journal*, *7*, 96–109.

Novellino, A., Scelfo, B., Palosaari, T., Price, A., Sobanski, T., Shafer, T. J., . . . Whelen, M. (2011). Development of micro-electrode array based tests for neurotoxicity: Assessment of interlaboratory reproducibility with neuroactive chemicals. *Frontiers in Neuroengineering*, *4*.

Otto, F., Goertz, P., Fleischer, W., & Siebler, M. (2003). Cryopreserved rat cortical cells develop functional neuronal networks on microelectrode arrays. *Journal of Neuroscience Methods*, *128*, 173.

Pare, D., Curro'Dossi, R., & Steriade, M. (1990). Neuronal basis of the Parkinsonian resting tremor: A hypothesis and its implications for treatment. *Neuroscience*, *35*(2), 217–226.

Pikovsky, A., Rosenblum, M., & Kurths, J. (2003). *Synchronization: A universal concept in nonlinear sciences*. Cambridge: Cambridge University Press.

Pikovsky, A. S., Rosenblum, M. G., Osipov, G. V., & Kurths, J. (1997). Phase synchronization of chaotic oscillators by external driving. *Physica D: Nonlinear Phenomena*, *104*(3), 219–238.

Rosenbaum, R., Tchumatchenko, T., & Moreno-Bote, R. (2014). Correlated neuronal activity and its relationship to coding, dynamics and network architecture. *Frontiers in Computational Neuroscience*, *8*, 102.

Satuvuori, E., Mulansky, M., Bozanic, N., Malvestio, I., Zeldenrust, F., Lenk, K., & Kreuz, T. (2017). Measures of spike train synchrony for data with multiple time scales. *Journal of Neuroscience Methods*, *287*, 25–38.

Selinger, J. V., Pancrazio, J. J., & Gross, G. W. (2004). Measuring synchronization in neuronal networks for biosensor applications. *Biosensors and Bioelectronics*, *19*(7), 675–683.

Shannon, C., & Weaver, W. (1948). A mathematical theory of communication. *Bell Syst. Tech. J.*, *27*(379), 623.

Sokal, D. M., Mason, R., & Parker, T. L. (2000). Multi-neuronal recordings reveal a differential effect of thapsigargin on bicuculline-or gabazine-induced epileptiform excitability in rat hippocampal neuronal networks. *Neuropharmacology*, *39*(12), 2408–2417.

Strogatz, S. (2000). From Kuramoto to Crawford: Exploring the onset of synchronization in populations of coupled oscillators. *Physica D: Nonlinear Phenomena*, *143*(1), 1–20.

Tass, P., Rosenblum, M. G., Weule, J., Kurths, J., Pikovsky, A., Volkmann, J., . . . Freund, H.-J. (1998). Detection of *n:m* Phase locking from noisy data: Application to magnetoencephalography. *Phys. Rev. Lett.*, *81*, 3291–3294.

Truccolo, W., Ahmed, O. J., Harrison, M. T., Eskandar, E. N., Cosgrove, G. R., Madsen, J. R., . . . Cash, S. S. (2014). Neuronal ensemble synchrony during human focal seizures. *Journal of Neuroscience*, *34*(30), 9927–9944.

Ward, L. M. (2003). Synchronous neural oscillations and cognitive processes. *Trends in Cognitive Sciences*, *7*(12), 553–559.

Witten, I., & Frank, E. (2000). *Data mining: Practical machine learning tools and techniques with Java implementations*. San Mateo, CA: Morgan Kaufmann.

Wong, R. O., Meister, M., & Shatz, C. J. (1993). Transient period of correlated bursting activity during development of the mammalian retina. *Neuron*, *11*(5), 923–938.

Received August 1, 2019; accepted January 8, 2020.